

## 4. Lateral-Torsional Buckling of Members in Bending

This chapter is devoted lateral-torsional buckling of members in bending. A first paragraph is devoted to a phenomenological description of the phenomenon. The second one collects a series of completely theoretical models derived for elastic beams of diverse cross section. Finally, a comprehensive discussion of the main code provisions is reported; both the Italian and the European codes are analyzed and applied.

### 4.1 Definitions and phenomenological description

Stability within the Euler definition has been already exposed in chapter 2 with reference to the case of members in compression. Under the two basic hypotheses of i) small displacements and ii) no imperfection, the behaviour of members in compression appeared as bifurcation problem whose solution is the trivial one under low level of axial load, switching to an adjacent one as the axial force approaches a particular critical value.

The same behaviour can be observed for members in bending; even in these cases, a critical value of the transverse load results in a bifurcation phenomenon: starting from the plane configuration characterizing the response of members in bending, an adjacent equilibrium configuration is assumed under that critical value. The possible adjacent configuration is usually described by out-of-plane displacements throughout the beam axis and a twisting angle (Figure 4.1).

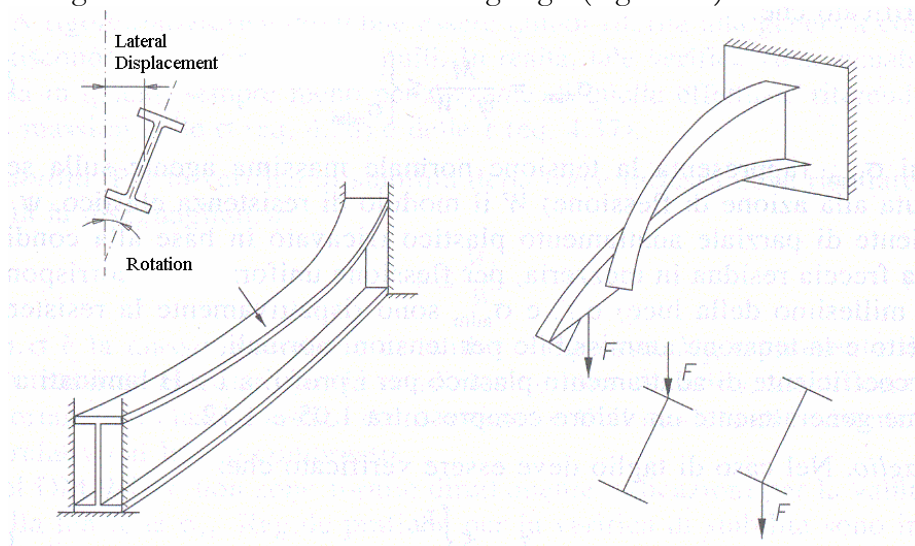


Figure 4.1: Lateral-torsional buckling for a cantilever beam.

As well as moments of inertia play a relevant role in affecting the buckling phenomenon under axial forces, other geometric properties of the transverse section result in getting the member more or less susceptible of lateral-torsional buckling. Lateral-torsional buckling of members in bending is also affected by load condition, being the phenomenon sensitive of the point of application of the transverse force throughout the section.

All these aspects of the lateral-torsional buckling phenomenon will be analyzed in the following. First of all a rather comprehensive explanation of the elastic theory will be given with some insights about the solution methods which can be utilized for obtaining approximate solution of the problem, being closed-form ones only available in few simple cases. Finally, both Italian Code and Eurocode 3 provisions for lateral-torsional buckling will be examined, commented and applied in some worked examples.

### 4.2 Theoretical insights

The theoretical study of the mentioned phenomenon starts from members with rectangular section, considering, in particular, the case of deep beams in which the two principal moments of inertia are significantly different; the case of more general sections will be also addressed with particular

focus on the I-shaped beams which are rather common in steel structures. The way in which the point of application of loads affects the behaviour of flexural members in terms of lateral-torsional buckling occurrence will be also examined; in particular, the difference in behaviour deriving by applying the transverse load either above, beneath or directly in the section centroid, will be also addressed. Influence of initial imperfection is also considered with the aim of understanding the behaviour of the so-called industrial member, with respect to the ideal case of perfectly straight ideal members.

#### 4.2.1 Lateral buckling of beams with rectangular section

Let us consider a beam of rectangular section whose principal radii of gyration are significantly different; in particular, the shorter one is referred to the out-of-plane bending as shown in Figure 4.2:

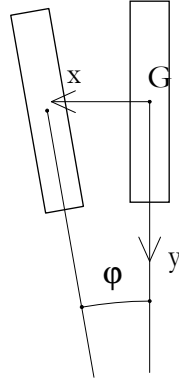


Figure 4.2: Adjacent lateral-torsional buckled configuration described by the twisting angle  $\varphi$

The twisting rotation  $\varphi$  which can possibly arise during the loading process results in a non perpendicular condition between the bending moment vector  $M$  (orthogonal to the bending plane) and the  $y$ -axis of the transverse section; consequently, the external bending moment is characterized by a non-zero component (approximately equal to  $M\varphi$ ) along the  $y$ -axis and, hence, an out-of-plane bending. If  $I_y$  is the moment of inertia with respect to the  $y$ -axis, the following Navier relationship can be stated between the bending moment and the resulting out-of-plane curvature:

$$EI_y \cdot \frac{d^2 u}{dz^2} = -M \cdot \varphi \quad (4.1)$$

where  $u=u(z)$  is the displacement component in  $x$  direction of the centroid  $G$  of the section at abscissa  $z$ .

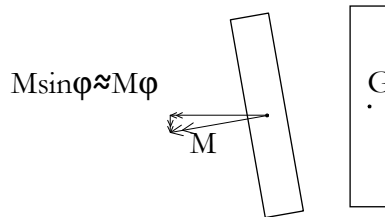


Figure 4.3: Bending moment in the two directions – Vertical plane

Lateral displacements possibly arising in the beam have also an influence on its torsional behaviour. Let us be  $GJ_t$  the torsional stiffness of the beam and consider a segmental part of the beam whose length is  $d\xi$  subjected to a bending moment  $M$  and a torsional one  $M_t$ .

According to the symbols introduced in Figure 4.3 the equilibrium equation to rotation in longitudinal direction can be easily written as follows:

$$-M_t + (M_t + dM_t) - M \cdot d\varphi = 0 \quad (4.2)$$

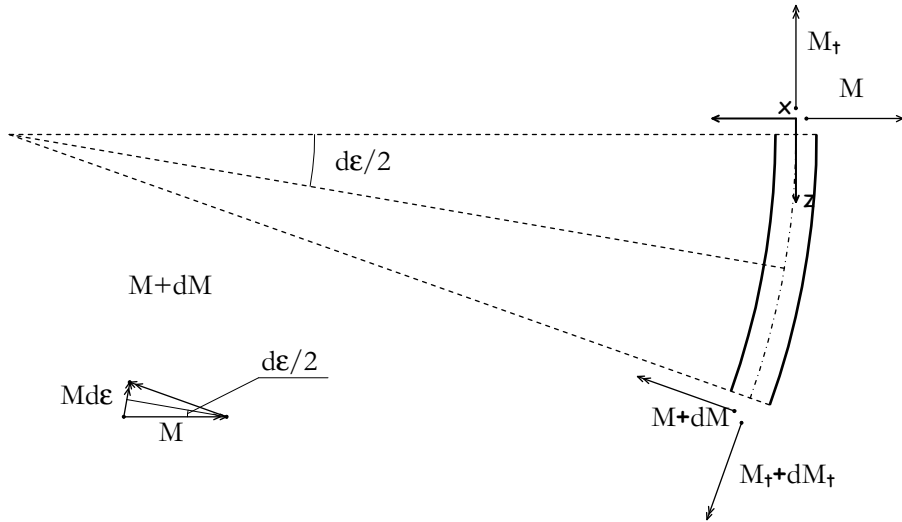


Figure 4.4: Relationship between torque and bending moment – Horizontal view

On the contrary, under the kinematical point of view, a simple relationship can be stated between the element length  $d\zeta$  (which can be approximated by the arc of length  $ds$ ) and the radius of curvature  $\rho_u$  of the beam axis in the horizontal plane:

$$d\epsilon = \frac{d\zeta}{\rho_u} \approx \frac{d^2 u}{d\zeta^2} \cdot d\zeta \quad (4.3)$$

The following equation can be obtained by substituting the (4.3) in (4.2) and expressing all quantities in terms of derivatives:

$$\frac{dM_t}{d\zeta} - M \cdot \frac{d^2 u}{d\zeta^2} = 0, \quad (4.4)$$

which, introducing equation (4.1) and expressing the torque  $M_t$  in terms of the unit angle of torsion according to the De Saint-Venant theory, leads to the following relationship between the twist angle  $\varphi(\zeta)$  and the corresponding bending moment  $M(\zeta)$ :

$$\frac{d}{d\zeta} \left[ GJ_t \frac{d\varphi}{d\zeta} \right] + \frac{[M(\zeta)]^2}{EI_y} \cdot \varphi = 0. \quad (4.5)$$

In the overwhelmingly common case of uniform transverse section, the above formula can be transformed in the following one, which is a second-order differential equation:

$$\frac{d^2 \varphi}{d\zeta^2} + \frac{[M(\zeta)]^2}{GJ_t \cdot EI_y} \cdot \varphi = 0. \quad (4.6)$$

The above equation is the well-known PRANDTL-MICHELL equation, who derived it in the nineteenth century.

## 4.2.2 Solution of some significant cases.

Equation (4.6) can be solved following different approaches, depending also by the transverse load applied throughout the beam length and the resulting bending moment function  $M(z)$ .

### 4.2.2.1 1<sup>st</sup> Case: Simply-supported beam under uniform bending moment $M(z)=M_0$ .

In this case the equation (4.6) has constant coefficients and, consequently, an easy closed-form solution can be found following the usual analytical methods for linear differential equations:

$$\frac{d^2 \varphi}{d\zeta^2} + \frac{M_0^2}{GJ_t \cdot EI_y} \cdot \varphi = 0 . \quad (4.7)$$

According to the mentioned end restraint conditions the general function describing the twisting rotation  $\varphi(\zeta)$  can be assumed in the following sinusoidal form:

$$\varphi(\zeta) = a_0 \cdot \sin\left(\frac{\pi \zeta}{L}\right) , \quad (4.8)$$

which can be properly regarded as the first term of the Fourier series of the real (and unknown) function  $\varphi(\zeta)$  (cosine terms are null as a result of the odd nature of the given function). Since the origin of the axes is placed at one of the two ends and, consequently,  $\zeta \in [0, L]$ , the equation comply with the restraint conditions in the case of simply-supported beams with rotational fixities at both ends.

Substituting equation (4.7) in (4.6), the following relationship can be obtained:

$$\left[ \left( \frac{\pi}{L} \right)^2 - \frac{M_0^2}{GJ_t \cdot EI_y} \right] \cdot a_0 \cdot \sin\left(\frac{\pi \zeta}{L}\right) = 0 , \quad (4.9)$$

and its left member vanishes for the non-trivial configuration (namely, if  $a_0 \approx 0$ ) if and only if the first factor does; consequently, the following critical value  $M_{0,cr}$  for the bending moment can be evacuate:

$$M_{0,cr} = \frac{\pi}{L} \cdot \sqrt{GJ_t \cdot EI_y} . \quad (4.10)$$

#### 4.2.2.2 2<sup>nd</sup> Case: Simply supported beam under uniformly distributed load.

In this case, assuming a reference system centred in the mid-span point, the bending moment can be easily expressed as follows:

$$M(\zeta) = \frac{qL^2}{8} \cdot (1 - \zeta^2) , \quad (4.11)$$

being  $\zeta \in [-1, 1]$  and the equation (4.6) has variable coefficients. Consequently, no-closed form solutions to be sought by analytical procedures are available and an alternative approximate method is needed. In particular, the Undetermined Coefficient Method can be utilized by introducing a power-series approximation of the unknown function considering separately even and odd exponents within the two terms  $\varphi_0$  e  $\varphi_1$  reflecting the nature of its component functions. A certain (even) number  $n$  of terms can be chosen for the power series and the expression of  $\varphi(z)$  can be placed in the following form:

$$\varphi(\zeta) = \varphi_0(\zeta) + \varphi_1(\zeta) = \sum_{i=0}^n A_i \zeta^i = \sum_{j=0}^{n/2} A_j \zeta^{2j} + \sum_{j=0}^{n/2} A_j \zeta^{2j+1} , \quad (4.12)$$

In the current case the function must be even in nature due to the structural symmetry and, hence, only the powers with even exponent can be considered:

$$\varphi(\zeta) = \varphi_0(\zeta) = \sum_{j=0}^{n/2} A_j \zeta^{2j} . \quad (4.13)$$

The non-dimensional abscissa  $\zeta$  can be easily introduced in terms as a function of the dimensional one  $\zeta$  as follows:

$$\zeta = \frac{\zeta - L/2}{L/2} \quad \text{and} \quad d\zeta = \frac{L}{2} \cdot d\zeta . \quad (4.14)$$

and the equation (4.6) can be written as follows:

$$\frac{d^2 \varphi}{d\zeta^2} + \frac{(qL^3/16)^2}{GJ_t \cdot EI_y} (1 - \zeta^2)^2 \cdot \varphi = 0 , \quad (4.15)$$

And introducing the following definition,

$$k^2 = \frac{(qL^3/16)^2}{GJ_t \cdot EI_y}, \quad (4.16)$$

results in the final form reported below:

$$\frac{d^2 \Phi}{d\zeta^2} + k^2 \cdot (1 - \zeta^2)^2 \cdot \Phi = 0, \quad (4.17)$$

Introducing equation (4.13) in (4.17), the maximum exponent of the various terms in  $\zeta$  is  $n+4$ . Collecting the terms corresponding characterized by the same power to the  $\zeta$  variable the following set of linear equation can be written in terms of the constants utilized for defining the above power series. In particular, a homogeneous set of  $n/2+1$  equations with the unknown  $A_{2j}$  ( $j=0 \dots n/2$ ) reported below (in the considered case  $n=20$ ) can be obtained:

$$\left\{ \begin{array}{l} A_0 k^2 + 2A_2 = 0 \\ 2A_0 k^2 - A_2 \cdot k^2 - 12A_4 = 0 \\ A_0 k^2 - 2A_2 k^2 + A_4 k^2 + 30A_6 = 0 \\ A_2 k^2 - 2A_4 k^2 + A_6 k^2 + 56A_8 = 0 \\ A_4 k^2 - 2A_6 k^2 + A_8 k^2 + 90A_{10} = 0 \\ A_6 k^2 - 2A_8 k^2 + A_{10} k^2 + 132A_{12} = 0 \\ A_8 k^2 - 2A_{10} k^2 + A_{12} k^2 + 182A_{14} = 0 \\ A_{10} k^2 - 2A_{12} k^2 + A_{14} k^2 + 240A_{16} = 0 \\ A_{12} k^2 - 2A_{14} k^2 + A_{16} k^2 + 306A_{18} = 0 \\ A_{14} k^2 - 2A_{16} k^2 + A_{18} k^2 + 380A_{20} = 0 \\ A_{16} k^2 - 2A_{18} k^2 + A_{20} k^2 = 0 \end{array} \right. \quad (4.18)$$

By the above set of  $n/2$  linear independent equations, the unknowns  $A_{2j}$  can be determined as a function of  $A_0$ , and can be substituted in equation (4.19) (in which  $\zeta$  has been replaced by  $z$ ) with the aim of obtaining  $\Phi$ :

$$\phi(\zeta) = A_0 \cdot \left( 1 - \frac{k^2 \zeta^2}{2} + \frac{k^2 \zeta^4}{6} + \frac{k^4 \zeta^4}{24} - \frac{k^2 \zeta^6}{30} - \frac{7k^4 \zeta^6}{180} - \frac{k^6 \zeta^6}{720} + \frac{13k^4 \zeta^8}{840} + \dots + \frac{k^{20} \zeta^{20}}{2432902008176640000} \right). \quad (4.19)$$

A suitable boundary condition has to be imposed to this expression of  $\phi(\zeta)$  considering that the twisting rotation vanishes at  $\zeta=1$ , due to the restraining effect of the rotational fixities:

$$\phi(1) = 0; \quad (4.20)$$

the above condition is always true for the trivial solution throughout all the beam axis and can be imposed to the solution (4.19) describing the laterally buckled configuration. In this second case, a critical value  $k_{cr}$  of the constant  $k$  can be determined obtaining the following approximate solution:

$$k_{cr} = \sqrt{\frac{(q_{cr} L^3 / 16)^2}{GJ_t \cdot EI_y}} = 1,7697, \quad (4.21)$$

from which the corresponding critical value  $q_{cr}$  of the uniformly distributed load  $q$  can be easily determined:

$$q_{cr} = \frac{16 \cdot k_{cr}}{L^3} \cdot \sqrt{GJ_t \cdot EI_y} = \frac{28,3152}{L^3} \cdot \sqrt{GJ_t \cdot EI_y} . \quad (4.22)$$

This solution has been assuming an approximated expression of the function  $\varphi(\zeta)$  involving the first 11 power terms of even exponent reported in equation (4.13). A wider sensitivity analysis has been carried out about the level of approximation which can be achieved by the numerical solution involving up to 20 power terms. Figure 4.5 shows the convergence of the numerical solution toward a stable value  $k_{cr}$  confirming the good approximation of the solution reported in equation (4.22).

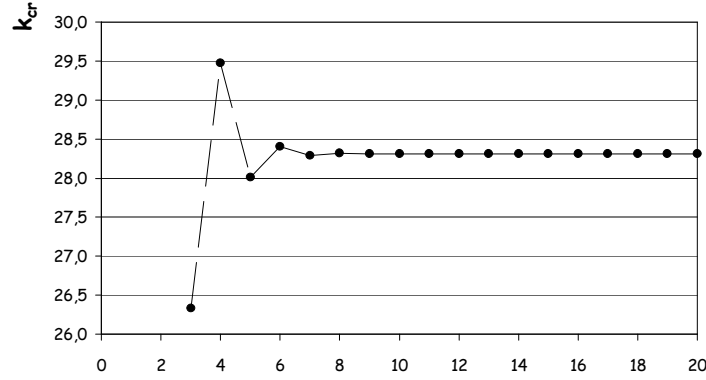


Figure 4.5: Value of  $k_{cr}$  as a function of the order  $n$  of approximation of the numerical solution.

The same figure shows that the same convergence process is generally non monotonic as the order of the approximating solution varies from 3 to 20.

#### 4.2.2.3 3<sup>rd</sup> Case: Simply-supported beam under a point load $Q$ at mid-span.

In this case the analytical expression of the bending moment, assuming that the non dimensional abscissa starts from the mid-span point, can be placed in the following form:

$$M(\zeta) = \frac{QL}{4} \cdot (1 - \zeta) , \quad (4.23)$$

with  $\zeta \in [-1, 1]$  and equation (4.6) has once more variable coefficients. The solution is sought following the same numerical approach utilized above assuming for  $\varphi(\zeta)$  a similar polynomial expression reported in (4.13). Following a similar procedure, the critical value  $Q_{cr}$  of the concentrated load  $Q$  can be derived as expressed below:

$$Q_{cr} = \frac{8 \cdot k_{cr}}{L^2} \cdot \sqrt{GJ_t \cdot EI_y} = \frac{11,8041}{L^2} \cdot \sqrt{GJ_t \cdot EI_y} . \quad (4.24)$$

#### 4.2.2.4 4<sup>th</sup> Case: Cantilever beam under uniform bending moment $M(z)=M_0$ .

In this case, equation (4.6) has constant coefficient

$$\frac{d^2 \varphi}{d\zeta^2} + \frac{M_0^2}{GJ_t \cdot EI_y} \cdot \varphi = 0 , \quad (4.25)$$

and, hence, a sinusoidal expression can be assumed for the general solution according to the imposed boundary conditions (rotational fixity at  $z=0$ ):

$$\varphi(\zeta) = \varphi_l \cdot \sin\left(\frac{\pi \zeta}{2L}\right) , \quad (4.26)$$

which can be, as usual, intended as the first term of the Fourier series of the unknown solution  $\varphi(z)$  (cosine coefficients are once more zero due to the particular boundary condition). Since the origin of

the reference system is at the fixed end of the beam. Introducing equation (4.7) in (4.6) the following relationship can be easily obtained:

$$\left[ \left( \frac{\pi}{2L} \right)^2 - \frac{M_0^2}{GJ_t \cdot EI_y} \right] \cdot a_0 \cdot \sin \left( \frac{\pi x}{2L} \right) = 0 , \quad (4.27)$$

which is true as  $a_0=0$ , or, in the non-trivial case, as the first factor in the square parentheses is zero and, consequently, the “critical” value  $M_{0,cr}$  of the bending moment  $M$  can be derived:

$$M_{0,cr} = \frac{\pi}{2L} \cdot \sqrt{GJ_t \cdot EI_y} , \quad (4.28)$$

#### 4.2.2.5 5<sup>th</sup> Case: Cantilever under uniformly distributed load.

Assuming the origin of the  $z$  axis at the free end of the cantilever, the function describing the bending moment can be expressed as follows:

$$M(z) = -\frac{q}{2} \cdot z^2 \Rightarrow M(\zeta) = -\frac{qL^2}{2} \cdot \zeta^2 , \quad (4.29)$$

in which the non dimensional abscissa  $\zeta = z/L$  has been conveniently introduced. The equation (4.6), can be, hence, written in the following form:

$$\frac{d^2\phi}{d\zeta^2} + \frac{(qL^3/2)^2}{GJ_t \cdot EI_y} (1-\zeta)^4 \cdot \phi = 0 , \quad (4.30)$$

or, equivalently,

$$\frac{d^2\phi}{d\zeta^2} + k^2 \cdot (1-\zeta)^4 \cdot \phi = 0 , \quad (4.31)$$

under the hypothesis that:

$$k^2 = \frac{(qL^3/2)^2}{GJ_t \cdot EI_y} . \quad (4.32)$$

Also in this case, a power series can be introduced for approximating the unknown solution; based on the nature of the problem and the choice of the relevant variables, the following approximation is introduced:

$$\phi(\zeta) = \phi_0(\zeta) = \sum_{j=0}^{n/2} A_j \zeta^{2j} . \quad (4.33)$$

Introducing (4.26) in (4.23), collecting the coefficients of the similar terms and imposing that a null product can be obtained if one of its factors is zero, the following homogeneous set of linear equation can be written (in the case of  $n=28$ ):

$$\left\{ \begin{array}{l} 2A_2 = 0 \\ 12A_4 = 0 \\ A_0k^2 + 30A_6 = 0 \\ A_2k^2 + 56A_8 = 0 \\ A_4k^2 + 90A_{10} = 0 \\ A_6k^2 + 132A_{12} = 0 \\ A_8k^2 + 182A_{14} = 0 \\ A_{10}k^2 + 240A_{16} = 0 \\ A_{12}k^2 + 306A_{18} = 0 \\ A_{14}k^2 + 380A_{20} = 0 \\ A_{16}k^2 + 462A_{22}k^2 = 0 \\ A_{18}k^2 + 552A_{24}k^2 = 0 \\ A_{20}k^2 + 650A_{26}k^2 = 0 \\ A_{12}k^2 + 756A_{28}k^2 = 0 \\ A_{24}k^2 = 0 \end{array} \right. . \quad (4.34)$$

The variables  $A_{2i}$  can be derived as a function of  $A_0$  and introducing them in equation (4.26) the following expression of the twisting rotation  $\phi(\zeta)$  can be obtained:

$$\phi(\zeta) = A_0 \cdot \left( 1 - \frac{k^2 \zeta^6}{30} + \frac{k^4 \zeta^{12}}{3960} - \frac{k^6 \zeta^{18}}{1211760} + \frac{k^8 \zeta^{24}}{668891520} \right). \quad (4.35)$$

As a boundary condition, the first derivative of  $\phi(\zeta)$  at the free end of the beam ( $\zeta=1$ ) have to be forced to zero. Consequently, a critical value  $k_{cr}$  of  $k$  can be deduced in the non trivial configuration, obtaining the following relationship:

$$k_{cr} = \sqrt{\frac{(q_{cr} L^3 / 2)^2}{GJ_t \cdot EI_y}} = 6,4278 , \quad (4.36)$$

and

$$q_{cr} = \frac{2 \cdot k_{cr}}{L^3} \cdot \sqrt{GJ_t \cdot EI_y} = \frac{12,8557}{L^3} \cdot \sqrt{GJ_t \cdot EI_y} , \quad (4.37)$$

or, in terms of global load:

$$Q_{cr} = q_{cr} \cdot L = \frac{12,8557}{L^2} \cdot \sqrt{GJ_t \cdot EI_y} , \quad (4.38)$$

or bending moment

$$M_{cr} = \frac{q_{cr} \cdot L^2}{2} = \frac{6,4277}{L} \cdot \sqrt{GJ_t \cdot EI_y} , \quad (4.39)$$

### 4.2.3 Influence of the transverse section shape: symmetric I-shaped profiles

Let us consider the symmetric I-shaped section whose depth is  $h$  and let  $\phi(z)$  be the twisting angle around the  $z$ -axis. The lateral displacement  $u$  (in  $x$ -direction) of the above flange can be related to the local value of the twisting angle as follows:



$$u(\zeta) = \frac{b}{2} \phi(\zeta) . \quad (4.40)$$

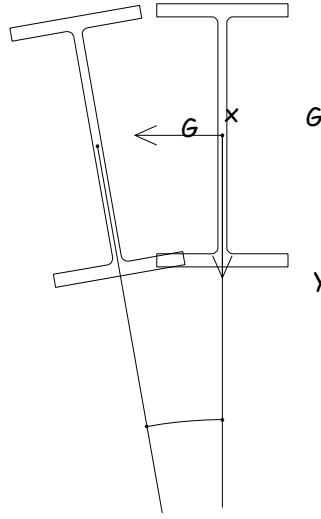


Figure 4.6: Symmetric I-shaped section.

Consequently, a curvature  $d^2u/dz^2$  arises throughout the axis of the flange and the corresponding bending moment in  $y$ -direction can be related to that curvature according to the usual linear relationship involving the relevant flexural stiffness:

$$\frac{d^2u}{d\zeta^2} = \frac{M_{1,y}}{EI_{y,f}} ; \quad (4.41)$$

By equilibrium, the shear force  $V_{1,y}$  orthogonal to the  $y$ -direction corresponds to the above bending moment  $M_{1,y}$ :

$$V_{1,y} = -\frac{dM_{1,y}}{d\zeta} \quad (4.42)$$

and, hence, a relationship between this shear force and the function describing the twisting angle  $\phi$  can be easily stated considering equations (4.8) and (4.9):

$$V_{1,y} = -EI_{y,f} \cdot \frac{b}{2} \cdot \frac{d^3\phi}{d\zeta^3} . \quad (4.43)$$

Since the force  $V_{1,y}$  acts on the above flange in the direction parallel to its axis and, for the same reasons, an opposite one is applied on the bottom flange, a secondary torque arises on the transverse section, whose sign is opposite to the one covered by the De Saint-Venant theory and mentioned above for the rectangular section:

$$M_{1,t} = V_{1,y} \cdot b = -\frac{1}{2} \cdot EI_{y,f} \cdot b^2 \cdot \frac{d^3\phi}{d\zeta^3} . \quad (4.44)$$

Consequently, the relationship between the torque and the twisting rotation  $\phi$  can be obtained by summing the De Saint-Venant contribution introduced in equation (4.5) and the further one described by equation (4.44):

$$M_t = -\frac{1}{2} \cdot EI_{y,f} \cdot b^2 \cdot \frac{d^3\phi}{d\zeta^3} + GJ_t \cdot \frac{d\phi}{d\zeta} . \quad (4.45)$$

Since the torque  $M_t$  stems out by the laterally buckle configuration and is consequently related to the bending moment, the following relationship reported in equation (4.4), can be stated between the two couples:

$$\frac{dM_t}{d\zeta} - M \cdot \frac{d^2u}{d\zeta^2} = 0 , \quad (4.46)$$

and, introducing equation (4.1) and (4.12), the following fourth-order differential equation in terms of  $\phi$  can be derived:

$$-\frac{1}{2} \cdot EI_{y,f} \cdot b^2 \cdot \frac{d^4 \phi}{d\zeta^4} + GJ_t \cdot \frac{d^2 \phi}{d\zeta^2} + \frac{[M(\zeta)]^2}{EI_y} \cdot \phi = 0, \quad (4.47)$$

and, finally,

$$-\frac{1}{2} \cdot \frac{EI_{y,f}}{GJ_t} \cdot b^2 \cdot \frac{d^4 \phi}{d\zeta^4} + \frac{d^2 \phi}{d\zeta^2} + \frac{[M(\zeta)]^2}{GJ_t \cdot EI_y} \cdot \phi = 0. \quad (4.48)$$

In a more general sense, the *warping moment of inertia* (or *sectorial moment of inertia*)  $I_\omega$  can be introduced, being in the case of symmetric I-shaped section:

$$EI_\omega = 2 \cdot EI_{y,f} \left( \frac{b}{2} \right)^2 = \frac{EI_{y,f} b^2}{2}, \quad (4.49)$$

and the general form of equation (4.45):

$$-EI_\omega \cdot \frac{d^4 \phi}{d\zeta^4} + GJ_t \cdot \frac{d^2 \phi}{d\zeta^2} + \frac{[M(\zeta)]^2}{EI_y} \cdot \phi = 0. \quad (4.50)$$

## 4.2.4 Solution of some significant cases.

### 4.2.4.1 1<sup>st</sup> Case: Simply-supported beam in uniform bending moment $M(z)=M_0$ .

Equation (4.45) has generally variable coefficients due to the fact the bending moment  $M(z)$  is related to the abscissa  $z$ . Far from being a practical representative case, uniform bending moment is a *cas d'école* in which the coefficient of the above equation are constant. Consequently, if  $M(z)=M_0$  equation (4.45) takes the following expression

$$-\frac{EI_\omega}{GJ_t} \cdot \frac{d^4 \phi}{d\zeta^4} + \frac{d^2 \phi}{d\zeta^2} + \frac{M_0^2}{GJ_t \cdot EI_y} \cdot \phi = 0, \quad (4.51)$$

and, as a sinusoidal expression is assumed for (the first terms of the Fourier series) the unknown function  $\phi(z)$

$$\phi(\zeta) = \phi_1 \cdot \sin \frac{\pi \zeta}{L}, \quad (4.52)$$

equation (4.46) can be transformed as follows:

$$\left[ -\frac{EI_\omega}{GJ_t} \cdot \left( \frac{\pi}{L} \right)^4 - \left( \frac{\pi}{L} \right)^2 + \frac{M_0^2}{GJ_t \cdot EI_y} \right] \cdot \phi_1 \cdot \sin \frac{\pi \zeta}{L} = 0. \quad (4.53)$$

A critical value  $M_{0,cr}$  of the uniform bending moment  $M_0$  resulting in lateral-torsional buckling of the considered beam can be defined as follows:

$$M_{0,cr} = \frac{\pi}{L} \cdot \sqrt{GJ_t \cdot EI_y} \cdot \sqrt{1 + \frac{EI_\omega}{GJ_t} \cdot \left( \frac{\pi}{L} \right)^2}. \quad (4.54)$$

It is straightforward to observe that equation (4.54) reduces to (4.10) for rectangular sections in which  $EI_\omega / GJ_t \cdot L^2 \rightarrow 0$ ; indeed, the latter equation provides a lower bound for the critical bending moment resulting, and equation (4.54) points out the stabilizing contribution of the flanges (and more generally of the terms  $EI_\omega / GJ_t \cdot L^2$ ) to lateral-torsional buckling occurrence.

In the case of a cantilever beam, equation (4.52) has to be replaced by the following expression which take accounts of the diverse restraint condition, forcing twisting rotation to vanish at the fixed end for  $z=0$ :

$$\phi(\zeta) = \phi_1 \cdot \sin \frac{\pi \zeta}{2L}. \quad (4.55)$$

The above equation, introduced in (4.50), and transformed as reported above with reference to a simply-supported beam, results in the following expression of the critical bending moment:

$$M_{0,cr} = \frac{\pi}{2L} \cdot \sqrt{GJ_t \cdot EI_y} \cdot \sqrt{1 + \frac{EI_\omega}{GJ_t} \cdot \frac{1}{4} \cdot \left(\frac{\pi}{L}\right)^2}, \quad (4.56)$$

even reducing to the corresponding equation (4.26) in the case of rectangular section, namely with  $EI_\omega/GJ_t \cdot L^2 \rightarrow 0$ .

Finally, comparing equations (4.54) and (4.56) the role of the different restraint condition on the two mentioned beams with respect to the reference case reproduced by equations (4.10) and (4.26) determined for the cases of rectangular section for simply-supported and cantilever beams, respectively.

#### 4.2.4.2 2<sup>nd</sup> Case: Trave semplicemente appoggiata con carico uniformemente distribuito $q$ .

The equation (4.50) can be transformed in the corresponding non-dimensional shape in terms of the non dimensional abscissa defined above:

$$-C \cdot \frac{d^4 \phi}{d\zeta^4} + \frac{d^2 \phi}{d\zeta^2} + k^2 (1 - \zeta^2)^2 \cdot \phi = 0, \quad (4.57)$$

where

$$k^2 = \frac{(qL^3/16)^2}{GJ_t \cdot EI_y} \quad C = 4 \cdot \frac{EI_\omega}{GJ_t \cdot L^2}. \quad (4.58)$$

.....

#### 4.2.5 Influence of the position of the point load on the transverse section

Within the previous paragraph, the loads are intended to be applied on the centroid  $G$  of the transverse section. Nevertheless, load can be also applied in other points of the section, above or beneath the centroid  $G$ . Figure 4.7 shows the case of a load applied in a point  $C$ , on the  $y$ -axis, at the distance  $d^*$  from the centroid  $G$  (assuming positive distances according to the direction of the  $y$ -axis).

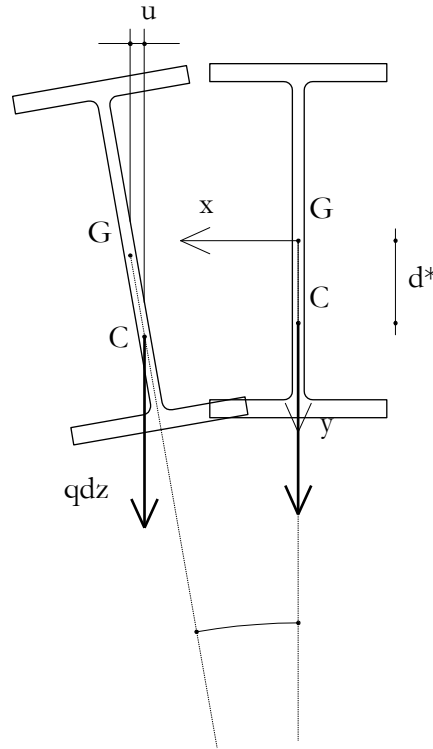


Figure 4.7: Symmetric I-shaped section with load applied in a general point  $C$

The eccentricity  $d^*$  results in a variation  $dM_t^*$  of the of the global torque acting on the transverse section which has to be added to the twisting moment expressed in equation (4.2):

$$dM_t^* = -qdz \cdot \phi d^*. \quad (4.59)$$

Coming back on the transformations leading from the equilibrium equation (4.2) to the final differential ones reported in equation (4.6) or (4.15) the effect induced by this moment variation can be easily understood.

In particular, considering equation (4.50), the following second-order differential equation can be derived taking account of the eccentricity  $d^*$  between G and C:

$$-\frac{EI_{\omega}}{GJ_t} \cdot \frac{d^4 \phi}{d\zeta^4} + \frac{d^2 \phi}{d\zeta^2} + \left[ \frac{[M(\zeta)]^2}{GJ_t \cdot EI_y} - \frac{qd^*}{GJ_t} \right] \cdot \phi = 0 . \quad (4.60)$$

#### 4.2.5.1 Simply supported beam under an uniformly distributed load $q$ .

As described in section 4.2.2.2, the expression of the bending moment in terms of a non-dimensional abscissa  $\zeta$ , whose origin is at mid-span of the beam, can be expressed as follows:

$$M(\zeta) = \frac{qL^2}{8} \cdot (1 - \zeta^2) , \quad (4.61)$$

being  $\zeta \in [-1, 1]$  and the equation (4.6) has variable coefficients. The simple case of rectangular section is considered ( $EI_{\omega}/GJ_t \cdot L^2 \rightarrow 0$ ) with the aim of pointing out the role of the distance  $d^*$ ; in that case equation (4.6) takes the following form:

$$\frac{d^2 \phi}{d\zeta^2} + \left[ \frac{[M(\zeta)]^2}{GJ_t \cdot EI_y} - \frac{qd^*}{GJ_t} \right] \cdot \phi = 0 . \quad (4.62)$$

and the following non-dimensional expression can be easily derived corresponding to equation (4.15) on the basis of the relationship (4.14):

$$\frac{d^2 \phi}{d\zeta^2} + \left[ \frac{(qL^3/16)^2}{GJ_t \cdot EI_y} (1 - \zeta^2)^2 - \frac{qd^*}{GJ_t} \right] \cdot \phi = 0 . \quad (4.63)$$

or, equivalently:

$$\frac{d^2 \phi}{d\zeta^2} + \frac{(qL^3/16)^2}{GJ_t \cdot EI_y} \cdot \left[ (1 - \zeta^2)^2 - \frac{4 \cdot EI_y}{qL^3} \cdot \frac{d^*}{b} \cdot \frac{b}{L} \right] \cdot \phi = 0 . \quad (4.64)$$

and the following parameter has been already introduced

$$k^2 = \frac{(qL^3/16)^2}{GJ_t \cdot EI_y} . \quad (4.65)$$

A further non-dimensional parameter  $k_1$  can be introduced considered depending on the quantities which controls the instability phenomenon, such as the  $EI_y/qL^3$  ratio, related to the flexural strain induced by the external load, the  $d^*/h$  and  $h/L$  ratios:

$$k_1 = \frac{4 \cdot EI_y}{qL^3} \cdot \frac{d^*}{b} \cdot \frac{b}{L} . \quad (4.66)$$

and, finally, the following expression can be obtained

$$\frac{d^2 \phi}{d\zeta^2} + k^2 \cdot \left[ (1 - \zeta^2)^2 - k_1 \right] \cdot \phi = 0 . \quad (4.67)$$

Equation (4.67) is formally similar to (4.17) and can be, hence, solved by considering a power series approximation of the unknown solution, considering  $n$  terms and obtaining  $n-1$  independent equations which can be used to express the value of the  $n-1$  constant as a function of  $A_0$ . In the present case the critical value  $k_{cr}$  depends also on the parameter  $k_1$ ; although no closed-form solutions can be found for  $k_{cr}$  or  $q_{cr}$  in the general case, the following one deals with the case of  $k_1=0$ , namely,  $d^*=0$ :

$$q_{cr} = \frac{16 \cdot k_{cr}}{L^3} \cdot \sqrt{GJ_t \cdot EI_y} = \frac{\gamma_{cr}}{L^3} \cdot \sqrt{GJ_t \cdot EI_y} . \quad (4.68)$$

Nevertheless, Figure 4.8 shows the values of the coefficient  $\gamma_{cr}$  determined through a numerical procedure as a function of  $k_1$ ; it is easy to verify that for  $k_1=0$  the same value reported in (4.68) can be found. On the contrary, the  $\gamma_{cr}$  value (namely the critical load  $q_{cr}$ ) hugely increases for  $k_1>0$  and, hence, for load applied beneath the centroid G, while decreases (although in a less sensitive way) for  $d^*<0$ . This apparent asymmetry of the problems is actually very limited, since the values of  $k_1$  of practical interest are in the neighbours of zero, ranging from -0,10 to 0,10, as one can easily check by considering (4.66) and the typical values of the parameters involved within the definition of  $k_1$ .

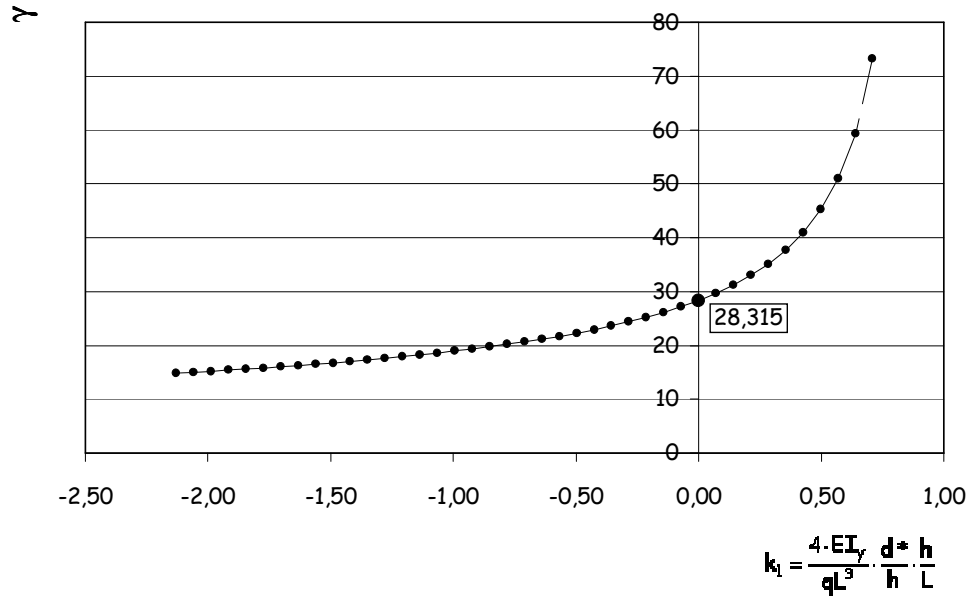


Figure 4.8: Values of  $\gamma_{cr}$  as a function of  $k_1$  defined by (4.66)

### 4.3 Code Provisions

The above theoretical models dealing with lateral-buckling for elastic members, can be usefully utilized for better understanding the provision of two codes of standards devoted to steel structures. As proposed in the previous section for flexural buckling under axial load, both Italian and European provisions will be discussed. Some worked examples will be also proposed for pointing out some practical aspects of those provisions.

#### 4.3.1 Italian Code (CNR 10011, DM96)

The mentioned Italian code proposes two alternative methods for checking flexural members against lateral-torsional stability:

- the  $\omega_1$ -method;
- the isolated flange method.

The first one is based on the definition of an amplification coefficient  $\omega_1$  for the normal stress in the compressed flange whose value is defined in terms of the beam depth-to-width and span-length-to-flange-thickness ratios. No details is given herein about that method for the sake of brevity and the interested reader can find further information on the code text.

On the contrary, the so-called isolated flange method is described in the following because of its significant meaningfulness under the mechanical standpoint. Indeed, the flange in compression is considered ad its slenderness is defined as the ratio between the effective span length  $L_0$  (defined according to the same rules described in the previous chapters depending on the end restraint conditions) and the transverse radius of inertia  $\rho_t$  which can be easily evaluated as follows:

$$\lambda_t = \frac{L_0}{\rho_t} . \quad (4.69)$$

The corresponding value of the  $\omega$  coefficient can be determined as a function of the transverse slenderness by utilizing either the stability curve  $c$  or  $d$  defined in section 2.8.1.1 for profiles respectively thinner or thicker than 40 mm.

The axial stress acting on the flange in compression has to be amplified by the above mentioned  $\omega$  coefficient as follows:

$$\sigma = \omega \cdot \frac{\frac{M_{eq}}{I_x} \cdot S_x}{A_f} \approx \omega \cdot \frac{M_{eq}}{I_x} y_G \leq f_{ad} \quad (4.70)$$

with the following meaning of the involved symbols:

- $A_f$  is the transverse area of the flange in compression;
- $I_x$  is the moment of inertia of the profile around the x-axis;
- $S_x$  is the static moment of the flange in compression with respect to the same axis;
- $y_G$  is the distance between the centroid G and the section edge in compression.

Furthermore,  $M_{eq}$  is the equivalent bending moment which depends on the shape of the bending moment diagram throughout the beam axis and can be assumed according to the same rules reported in section 2.8.1.1.

Finally, it is worth noticing that, according to equation (4.70), the lateral-torsional buckling occurrence can be intended as the out-of-plane flexural buckling of the section flange in compression.

### 4.3.2 European Code (EC 3)

The EC3 formulation of the lateral-torsional stability check of members in bending is more general as well as much more formally complex. The external relationship to be checked for verifying the member in bending against the onset of lateral-torsional buckling phenomenon is reported below:

$$M_{b,Rd} = \chi_{LT} \beta_w W_{pl,y} \frac{f_{ay}}{\gamma_{M1}} \quad (4.71)$$

where further symbols have been introduced. In particular,  $W_{pl,y}$  is the plastic modulus around the transverse axis (according to the EC3 assumption  $y$ - $y$  and  $\bar{x}$ - $\bar{x}$  are the two main centroidal axis as represented in Figure 2.19). Furthermore, the  $\beta_w$  factor can be defined as follows depending on the class of the transverse section:

- Class 1 and 2:  $\beta_w = 1$ ;
- Class 3:  $\beta_w = W_{el,y} / W_{pl,y}$ ;
- Class 4:  $\beta_w = W_{eff,y} / W_{pl,y}$ ;

with the same meaning of the symbols already introduced in chapter 2. The reduction factor  $\chi_{LT}$  takes into account the effect of lateral slenderness on the occurrence of the lateral-torsional buckling. A similar definition to that provided by equation (2.75) for the reduction factor  $\chi$ , can be utilized for  $\chi_{LT}$ :

$$\chi_{LT} = \frac{1}{\Phi_{LT} + \sqrt{\Phi_{LT}^2 - \bar{\lambda}_{LT}^2}} \quad (4.72)$$

where  $\bar{\lambda}_{LT}$  is the relative slenderness which even control the value of  $\Phi_{LT}$  according to the following function

$$\Phi_{LT} = 0.5 \cdot \left[ 1 + \alpha_{LT} \cdot (\bar{\lambda}_{LT} - 0.2) + \bar{\lambda}_{LT}^2 \right] \quad (4.73)$$

The parameter  $\alpha_{LT}$  represents an imperfection coefficient and its value can be assumed as follows:

- hot-rolled section  $\alpha_{LT} = 0.21$ ;
- hot-rolled section  $\alpha_{LT} = 0.49$ .

The relative (or non-dimensional) slenderness  $\bar{\lambda}_{LT}$  is defined as the square root of the ratio between the ultimate flexural strength of the transverse section (namely, the plastic moment for profiles

in classes 1 and 2, the yielding moment for profiles in class 3 and the effective one for profiles in class 4) and the elastic lateral-buckling moment  $M_{cr}$ :

$$\bar{\lambda}_{LT} = \sqrt{\frac{\beta_w \cdot W_{pl,y} \cdot f_{ay}}{M_{cr}}} . \quad (4.74)$$

The parameters affecting the critical moment resulting in lateral-torsional buckling for elastic members have been pointed out in the first section on the present paragraph. The following general relationship can be assumed the transverse section of whichever shape:

$$M_{cr} = C_1 \frac{\pi^2 EI_{\tilde{z}}}{(kL)^2} \cdot \left( \sqrt{\left( \frac{k}{k_w} \right)^2 \cdot \frac{I_w}{I_{\tilde{z}}} + \frac{(kL)^2 GJ_t}{\pi^2 EI_{\tilde{z}}} + (C_2 \tilde{z}_g)^2} - C_2 \tilde{z}_g \right), \quad (4.75)$$

where the symbols have the meaning described below:

- $\tilde{z}_g$  is the distance between the section centroid G and the actual point of application of the loads. It is assumed being positive if the load is applied above the centroid and, hence, the following relationship can be recognized with one of the parameters introduced in section 4.2.5:  $\tilde{z}_g = -d^*$ ;
- the factor  $k_w$  is the coefficient related to the effective length of the beam with respect to the restraints to warping (namely, the possible deformation of the transverse section with respect to its plane). The value 0.5 is assumed for the double fix ends, while the value 1.0 is given in the case of free warping at the end. Finally, 0.7 can be assumed if warping is restrained on one end and free on the other one;
- the factor  $k$  takes account of the end restraints in terms of twisting rotation. The value 0.5 corresponds to full restraints, 1.0 to completely free scheme and finally 0.7 can be taken in the intermediate situation;
- the parameter  $J_t$  is torsional stiffness;
- the parameter  $I_{\tilde{z}}$  is moment of inertia around the weak axis ( $I_y$  throughout the previous section devoted to the theoretical bases);
- the parameter  $I_w$  is the so-called warping constant which is a sort of second moment of the moments of inertia. For the doubly symmetric I-shaped sections, the following relationship exists between  $I_w$  and  $I_z$ :

$$I_w = \frac{I_{\tilde{z}} \cdot (b - t_f)^2}{4} . \quad (4.76)$$

- $L$  is the beam span length;
- the constants  $C_1$  and  $C_2$  can be taken by Table 4.1 and Table 4.2 depending on the shape of the bending moment diagram throughout the beam axis.

With the aim of better clarifying the meaning of the factors  $k$  and  $k_w$ , Figure 4.9 shows different restraining conditions regarding twisting rotation and warping.

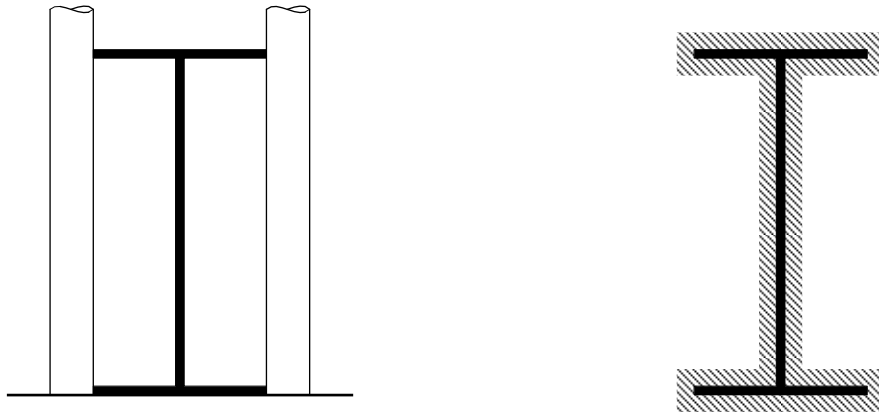


Figure 4.9: Different restraint condition on twisting rotation and warping

The general equation (4.75) can be simplified in some cases of practical interest such as:

- transversal load applied on the centroidal point G (which for doubly symmetric profiles coincides with the shear centre):

$$M_{cr} = C_1 \frac{\pi^2 EI_{\tilde{z}}}{(kL)^2} \cdot \left( \sqrt{\left( \frac{k}{k_W} \right)^2 \cdot \frac{I_W}{I_{\tilde{z}}} + \frac{(kL)^2 GJ_t}{\pi^2 EI_{\tilde{z}}}} \right), \quad (4.77)$$

- fully fixed beam with transversal load applied in G:

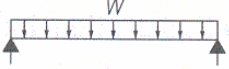
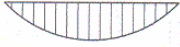
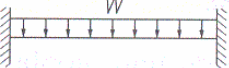

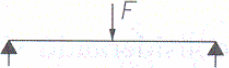

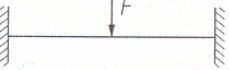

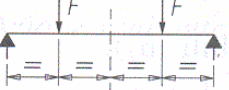

$$M_{cr} = C_1 \frac{\pi^2 EI_{\tilde{z}}}{(kL)^2} \cdot \left( \sqrt{\frac{I_W}{I_{\tilde{z}}} + \frac{(kL)^2 GJ_t}{\pi^2 EI_{\tilde{z}}}} \right), \quad (4.78)$$

Table 4.1: Coefficients of equivalent uniform moment for linear diagrams (end forces).

Load Condition	Bending Moment diagram	k	Coefficients		
			C <sub>1</sub>	C <sub>2</sub>	C <sub>3</sub>
		1,0 0,7 0,5	1,000 1,000 1,000	—	1,000 1,113 1,144
		1,0 0,7 0,5	1,141 1,270 1,305	—	0,998 1,565 2,283
		1,0 0,7 0,5	1,323 1,473 1,514	—	0,992 1,556 2,271
		1,0 0,7 0,5	1,563 1,739 1,788	—	0,977 1,531 2,235
		1,0 0,7 0,5	1,879 2,092 2,150	—	0,939 1,473 2,150
		1,0 0,7 0,5	2,281 2,538 2,609	—	0,855 1,340 1,957
		1,0 0,7 0,5	2,704 3,009 3,093	—	0,676 1,059 1,546
		1,0 0,7 0,5	2,927 3,009 3,093	—	0,366 0,575 0,837
		1,0 0,7 0,5	2,752 3,063 3,149	—	0,000 0,000 0,000



Table 4.2: Coefficients of equivalent uniform moment for general cases (distributed loads).

Load and End Restraint Conditions	Bending Moment Diagram	$k$	Coefficients		
			$C_1$	$C_2$	$C_3$
		1,0 0,5	1,132 0,972	0,459 0,304	0,525 0,980
		1,0 0,5	1,285 0,712	1,562 0,652	0,753 1,070
		1,0 0,5	1,365 1,070	0,553 0,432	1,730 3,050
		1,0 0,5	1,565 0,938	1,267 0,715	2,640 4,800
		1,0 0,5	1,046 1,010	0,430 0,410	1,120 1,890

## 4.4 Worked examples

The following examples are proposed for pointing out some practical aspects related to lateral-torsional stability checks in steel beams in bending.

### 4.4.1.1 Lateral torsional stability check simply supported beam

Let us consider the simply supported beam in Figure 4.10 under the following uniformly distributed loads:

- Dead Load  $g_k = 9.0 \text{ kN/m}$ ;
- Live Load  $q_k = 6.0 \text{ kN/m}$ ;

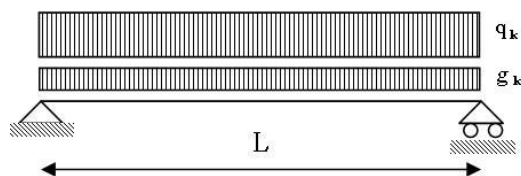


Figure 4.10: Simply supported beam with torsional end restraints.

The transverse section of the beam is realized by a standard IPE270 profile whose key geometric properties are listed below (steel grade S235):

- depth  $h$  270 mm;
- width  $b$  135 mm;
- flange thickness  $t_f$  10.2 mm;
- web thickness  $t_w$  6.6 mm;
- chord radius  $r$  15 mm;

- section area	A	45.94 cm <sup>2</sup> ;
- self-weight per unit length	g <sub>k</sub>	0.35 kN/m;
- moment of inertia around the strong axis	I <sub>y</sub>	5790 cm <sup>4</sup> ;
- moment of inertia around the weak axis	I <sub>z</sub>	420.0 cm <sup>4</sup> ;
- torsional constant	J <sub>t</sub>	15.94 cm <sup>4</sup> ;
- warping constant	I <sub>w</sub>	0.071 cm <sup>6</sup> ;
- plastic modulus around the strong axis	W <sub>pl,y</sub>	484.0 cm <sup>3</sup> ;
- plastic modulus around the weak axis	W <sub>pl,z</sub>	96.95 cm <sup>3</sup> ;
- span length	L	6.00 m.

#### 4.4.1.1.1 Lateral-torsional stability check according to the Italian Code provisions.

The isolated-flange method can be utilized for carrying out the safety check against lateral-torsional buckling according to the Italian Code provisions. The procedure follows the steps reported below:

##### Step #1: evaluation lateral slenderness of the flange in compression:

Since rotational restraints are considered at both ends the effective length (evaluated taking only account of the rotational restraints) is  $L_0=L/2$ . Moreover, the out-of-plane radius of gyration of the profile flange can be easily evaluated

$$\rho_t = \frac{b}{\sqrt{12}} = \frac{135}{\sqrt{12}} = 38.97 \text{ mm} , \quad (4.79)$$

and the corresponding slenderness is:

$$\lambda_t = \frac{L_0}{\rho_t} = \frac{3000}{38.97} = 76.98 . \quad (4.80)$$

Finally, the plastic slenderness can be evaluated as follows:

$$\lambda_p = \pi \sqrt{\frac{E_a}{f_{ay}}} = \pi \sqrt{\frac{210000}{235}} = 93.91 . \quad (4.81)$$

##### Step #2: evaluation of the $\omega$ factor:

Since the flange stiffness is smaller than 40 mm the curve  $c$  mentioned in section 2.8.1 has to be considered. The non-dimensional slenderness  $\lambda_t/\lambda_p = 0.81$  leads to the following value for the  $\omega$  factor:

$$\omega = 1.540 , \quad (4.82)$$

##### Step #3: evaluation of the compressive stress in the flange:

The maximum bending moment throughout the beam axis can be easily evaluated as follows:

$$M_{max} = \frac{(\gamma_g (g_k + g'_k) + \gamma_q q_k) \cdot L^2}{8} = \frac{(1.4 \cdot (0.35 + 9.0) + 1.5 \cdot 6.0) \cdot 6^2}{8} = 99.4 \text{ kNm} , \quad (4.83)$$

and the following mean value can be assumed because of the sinusoidal shape of the bending moment diagram:

$$M_m = \frac{2}{3} \cdot M_{max} = \frac{2}{3} \cdot 99.4 = 66.26 \text{ kNm} , \quad (4.84)$$

and the equivalent moment is

$$M_{eq} = 1.3 \cdot M_m = 1.3 \cdot 66.26 = 86.14 \text{ kNm} , \quad (4.85)$$

which is included within the range  $[0.75 M_{max}, M_{max}]$ .

Since the flange thickness is negligible with respect to the beam depth, the approximation in equation (4.70) is acceptable (being on the conservative side) and the following value of the compressive stress can be evaluated.

$$\sigma = \omega \cdot \frac{\frac{M_{eq}}{I_x} \cdot S_x}{A_f} = 1,540 \cdot \frac{\frac{86.14 \cdot 10^6}{5.8 \cdot 10^7} \cdot \frac{135 \cdot 10.2}{2} \cdot (135 - 5.1)}{135 \cdot 10.2} = 297.10 \text{ MPa} \geq f_{ad} = 235 . , \quad (4.86)$$

and the stability check against lateral-torsional buckling is not satisfied.

#### 4.4.1.1.2 Lateral-torsional stability check according to the EC3 provisions.

The same exercise can be also faced within the framework of the EC3 provisions which can be applied following step-by-step the formulae reported in section 4.3.2.

##### Step #1: classifying the transverse section:

Since the adopted steel grade is  $f_y=235$  MPa, the value  $\epsilon=1$  can be assumed for the parameter mentioned in Table 2.3 and Table 2.4. The following values of the length-to-thickness ratios can be evaluated for flange and web:

- flange  $c/t_f=(135/2)/10.2=6.6 \leq 10$  Class 1;
- web  $d/t_w=(270-2 \cdot 10.2-2 \cdot 15)/6.6=33.3 \leq 72$  Class 1

Finally, the profile IPE270 made out of steel S235 is in class 1 if loaded in bending.

##### Step #2: evaluating the critical moment for the elastic beam:

According to the assumed hypotheses on the transverse section and the end restraint conditions, the following values can be assumed for the parameters involved in equation (4.77) which can be properly considered because the transverse load is applied of the shear centre (namely, the centroid G) of the transverse section:

- $C_1=0.972$ ;
- $k=0.5$ ;
- $k_w=1.0$ ;

and the critical moment can be derived by the mentioned relationship:

$$M_{cr} = 0.972 \cdot \frac{\pi^2 210000 \cdot 4200000}{(0.5 \cdot 6000)^2} \cdot \left( \sqrt{\left( \frac{0.5}{1.0} \right)^2 \cdot \frac{7.06 \cdot 10^{10}}{4200000} + \frac{(0.5 \cdot 6000)^2 80770 \cdot 159400}{\pi^2 210000 \cdot 4200000}} \right) = , \quad (4.87)$$

$$= 124.41 \cdot 10^6 \text{ Nmm} = 124.41 \text{ kNm}$$

##### Step #3: evaluating the non dimensional lateral slenderness:

According to the definition provided in equation (4.74), the value of the non-dimensional slenderness can be easily quantified:

$$\bar{\lambda}_{LT} = \sqrt{\frac{\beta_w \cdot W_{pl,y} \cdot f_{ay}}{M_{cr}}} = \sqrt{\frac{1.0 \cdot 484000 \cdot 235}{124.41 \cdot 10^6}} = 0.956 . \quad (4.88)$$

##### Step #4: evaluating the reduction factor $\chi_{LT}$ :

The term  $\Phi_{LT}$  has to be firstly determined as a function of the non-dimensional slenderness and the imperfection coefficient  $\alpha_{LT} = 0.21$ :

$$\begin{aligned} \Phi_{LT} &= 0.5 \cdot \left[ 1 + \alpha_{LT} \cdot (\bar{\lambda}_{LT} - 0.2) + \bar{\lambda}_{LT}^2 \right] = \\ &= 0.5 \cdot \left[ 1 + 0.21 \cdot (0.956 - 0.2) + 0.956^2 \right] = 1.036 . \end{aligned} \quad (4.89)$$

Consequently, the following value of the reduction factor can be derived according to equation (4.72):

$$\chi_{LT} = \frac{1}{1.107 + \sqrt{1.107^2 - 1.021^2}} = 0.696 , \quad (4.90)$$

##### Step #5: evaluating design value of the resisting moment $M_{b,Rd}$ :

The bending moment resulting in the occurrence of the lateral-torsional buckling phenomenon can be easily evaluated as a design value according to equation (4.71):

$$\begin{aligned} M_{b,Rd} &= \chi_{LT} \beta_w W_{pl,y} \frac{f_{ay}}{\gamma_{M1}} = 0.696 \cdot 1.0 \cdot 484000 \cdot \frac{235}{1.05} = \\ &= 75.34 \cdot 10^6 \text{ Nmm} = 75.34 \text{ kNm} \end{aligned} \quad (4.91)$$

which is greater than the corresponding external moment  $M_{sd} = M_{max} = 99.4 \text{ kNm}$ . Consequently, the lateral-torsional stability check is not satisfied neither according to the EC3 provisions.

## 4.5 Unworked examples

The following exercises are left to the readers:

- 1) for the same beam reported in paragraph 4.4.1.1.1, what is the maximum value of the live loads  $q_k$  for the beam to comply with the lateral-torsional stability check according to the Italian Code provisions?;
- 2) for the same beam reported in paragraph 4.4.1.1.1, what is the maximum span length for the beam to comply with the lateral-torsional stability check according to the Italian Code provisions?;
- 3) for the same beam reported in paragraph 4.4.1.1.1, design the transverse section to comply with the lateral-torsional stability check according to the Italian Code provisions;
- 4) for the same beam reported in paragraph 4.4.1.1.2, evaluate the resisting moment  $M_{b,Rd}$  against the lateral-torsional buckling phenomenon considering that the same loads acts either at the bottom (case 1) or the top (case 2) of the section;
- 5) for the same beam reported in paragraph 4.4.1.1.2, perform the same lateral stability check with reference to a steel grade S355;
- 6) for the same beam reported in paragraph 4.4.1.1.2, perform the same lateral stability check considering a cantilever scheme with length  $L=3.00 \text{ m}$ .